Bird Strike and Novel Design of Fan Blades

Syed Noman Husainie

Aventec Inc. & University of Toronto

***Abstract**: The intent of this project was to find an appropriate bird substitute model and evaluate how engine blade properties can be tweaked to better handle bird strikes. Several bird geometries and material models were evaluated using the Lagrangian and smoothed particle hydrodynamic (SPH) modeling approaches. The SPH method was found to be more efficient for modeling a bird. All simulations were performed using Abaqus 2016. The material model for the calibrated bird model was best represented using a tabulated equation of state with 10% porous gelatin. The results for the hemispherical-ended cylinder with a length-to-diameter ratio of 1.6 correlated well with experimental results. Bird impact simulations on various blade geometries showed that increasing the blade twist for a rotating blade would improve its impact performance. It's recommended that leading edges of an engine blade are kept solid. Regions away from the leading edge may adopt a sandwich configuration to minimize weight.*

***Keywords**: Aircraft, Bird Strike, CAE, Coupled Analysis, Damage, Engine Fan Blade, Equation of State, Foreign Body Impact, Implicit-Explicit Coupling, Preload, Smoothed Particle Hydrodynamics.*

1. Introduction

Bird strikes are an important phenomenon that must be taken into consideration for aircraft design. Between 1988 and 2012, 250 people were killed and over 229 aircraft were destroyed because of bird strikes (Federal Aviation Administration, 2013). It is estimated that bird strike accidents cost the US civil aviation industry approximately $495 million per year. Furthermore, nearly 77% of the major bird strike incidents can be attributed to engine ingestion (Cleary et al., 2005). As engines are the only thrust providing mechanisms for the aircraft, it is critical to investigate and mitigate the effects of bird strikes on engines.

Bird strikes have been reported since the early days of flight and date back to as early as 1908, when Orville Wright struck a flock of birds. The earliest fatal bird strike accident happened in 1912, when a gull got stuck in the flight controls of a Wright Flyer, killing the pilot Cal Rodgers (Cleary et al., 2005). Bird strikes have continued to increase since then and this can be attributed to the increase in the population of large bird species, increase in air travel, and the shift towards less and quieter engines on aircraft.

To address the concerns of bird strikes on engines, engine manufacturers must go through physical testing to ensure that in the event of a foreign body ingestion, the engine can provide sufficient thrust so that the aircraft can land safely at normal operating speeds. Specifically, for a single large bird, the Federal Aviation Administration (FAA) states that engines must be tested for various bird sizes depending on the inlet throat area. For large engines of inlet areas more than and equal to

3.90 m^2, a bird of mass 3.65 kg must be tested for ingestion. Several other ingestion requirements exist for different parts of the aircraft in various conditions.

Currently, the only way to certify components with regards to bird impact is by performing a physical test. This involves firing an actual bird carcass or a gelatin model of the bird towards an engine and determining the damage to the engine. This is an expensive process as several tests may be required to evaluate the effectiveness of the engine. The goal thus is to replace the expensive physical testing by computer simulations. If simulations of bird strikes are accurately able to predict the behavior of bird strikes on engines, then the engine design can be optimized before an actual physical test is carried out. This will lower the costs and expedite the design and certification processes.

1.1 Objectives of the Study

The scope of the project was designed to meet the following objectives:

i. To develop an appropriate finite element bird model that accurately captures the response of a bird strike on an aircraft.

ii. To evaluate the robustness of various finite element techniques that can be used to model the high-speed impact of soft bodies.

iii. To suggest an engine blade design which can better handle the impact of a bird strike.

This paper will outline a workflow of the methods that may be employed to perform a bird strike impact analysis on an aircraft engine blade. Furthermore, the paper will also outline some of the techniques which may be used to optimize the shape of engine blades such that they are better suited to handle soft body impacts.

1.2 Method of Approach

Several finite element models of the bird were created and tested on a rigid target. Bird properties including shape, material, and mass were varied and the finite element results were compared with theoretical and experimental data available in literature. Mesh sensitivity analysis was also performed. The Lagrangian and Smoothed Particle Hydrodynamics (SPH) approaches were evaluated to determine which formulation yields better results. Once good correlations were observed, the selected bird model and finite element approach was used to study the impact of bird strikes on deformable engine blades. Blade geometrical properties were varied to understand how the blade design can be changed to better handle bird impacts.

2. Bird Model

It is well documented that the behavior of birds impacting a rigid target may be approximated using a hydrodynamic material model (Barber et al., 1978). Specifically, at high-speed impacts the bird behaves like a fluid with negligible viscosity (Wilbeck, 1977). Experimental studies have also found that an actual bird strike may be represented by modeling the bird as a circular cylinder with the same mass, density, and compressibility as the real bird.

Bird impact behavior on rigid targets can be divided into four main stages, namely the initial shock stage, pressure decay stage, steady state stage, and the pressure termination stage (Figure 1).

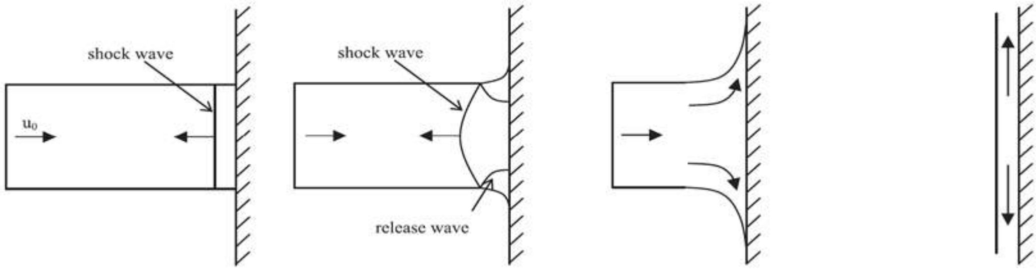

(a) Initial shock (b) Pressure decay (c) Steady state (d) Pressure termination

Figure 1. Illustration of soft body impact phases as described by Wilbeck (Wilbeck, 1977; Heimbs, 2011).

In the first stage, the bird impacts a surface with an initial velocity, u_0. The material near the surface is instantaneously brought to rest, which creates a shock wave (called the Hugoniot shock). This shock wave is parallel to the surface of impact and propagates down the bird's body. The initial pressure peak at the impact point is called the Hugoniot pressure, P_H.

The shock wave results in a significant pressure difference on the surface. This results in material flow on the un-impacted free surface. As the material accelerates outwards, a release wave is formed, which propagates towards the center of the impact, interacting with the shock wave. The interaction decreases the pressure at the impact point and represents the second stage of impact.

After several cycles of the release waves interacting with shock waves, the material begins to flow steadily. The existence of steady flow depends on the length/diameter ratio of the bird model. For a straight-ended cylinder a ratio of 2 ensures that the complete steady flow regime is observed for most impact velocities (Wilbeck, 1977).

The pressure continues to decrease as the release waves interact with the shock wave. Eventually steady flow is established at which point the material flows entirely radial. In this regime, a steady stagnation point is reached, which has a maximum at the center of impact.

2.1 Calculation of Hugoniot and Stagnation Pressures

The theoretical shock pressure in a bird strike can be found by applying the conservation laws of mass and momentum across a standing one-dimensional shock. The Hugoniot pressure can then be defined as the following.

$$P_H = \rho_1 u_s u_0 \tag{1}$$

The shock velocity for most solids and fluids can be found using the linear Hugoniot relationship (Wilbeck, 1977).

$$u_s = c_0 + k u_p \tag{2}$$

For the impact of a soft body on a rigid plate, the particle velocity u_p is equal to the impact velocity, u_0. For water the constant k in the above equation is 2, while the speed of sound c_0 in water is defined as 1482.9 m/s. The above relationship has been found to be a reasonable approximation for water, up to speeds of Mach 1.2 (Heymann, 1968). When applied to the bird impact study, the density ρ_0, represents the initial density of the bird before impact, u_0 represents the impact velocity, and u_s represents the shock wave velocity.

Once steady state is reached, the flow pressure P_s can be calculated using the Bernoulli relationship (Wilbeck, 1977). This assumption is applicable for incompressible flow. Furthermore, the bird material is able to reach steady flow conditions due to the very high stresses observed during impact compared to the bird's material strength.

$$P_s = \frac{1}{2}\rho_0 u_0^2 \quad (3)$$

The total time t_D needed for the impact to reach the pressure termination stage can be calculated using the following equation, where L represents the material's length before impact.

$$t_D = \frac{L}{u_0} \quad (4)$$

Based on the research by Wilbeck and other simulations performed in literature, the duration of the stagnation or steady flow stage can be reasonably approximated to exist between ${}^{1}/_{3}\,t_D$ – ${}^{2}/_{3}\,t_D$ (Airoldi & Cacchione, 2006). This stagnation pressure can then be expressed with respect to t_D.

$$P_s = \frac{\int_{{}^{1}/_{3}t_D}^{{}^{2}/_{3}t_D} P\,dt}{{}^{2}/_{3}\,t_D - {}^{1}/_{3}\,t_D} \quad (5)$$

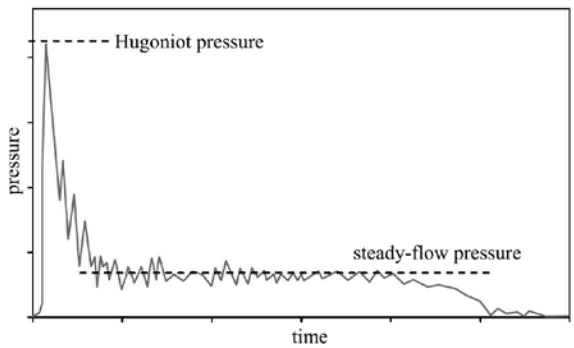

Figure 2. Typical variation with time during a high-speed bird impact on a rigid plate (Heimbs, 2011).

2.2 The Effects of Porosity

The effect of porosity on soft body impacts was explored extensively by Barber et al. and Wilbeck (Barber et al., 1978; Wilbeck, 1977). The need for analyzing porous materials for the purposes of bird impact studies arises from the development of an appropriate substitute material for modeling bird strikes. The addition of porosity requires the theory discussed earlier to be modified. Specifically, the linear Hugoniot relationship fails to hold for porous materials. Generally stated however, porosity influences both the compressibility and the shock velocity of a material during impact. The effects of compressibility at higher velocities tend to increase the steady flow pressures observed. The density of a porous material, ρ_z, can be approximated using the fraction of porosity, z.

$$\rho_z = z\rho_{air} + (1-z)\rho_f \tag{6}$$

In the previous equation, ρ_f represents the density of the non-porous medium, while ρ_{air} represents the density of the void material, which in this case is being assumed to be air.

2.3 Bird Material Model

Several different methods exist to model the material behavior of birds. Typically, the material behavior of birds has been modelled using an elastic-plastic hydrodynamic material model. Such a model relates the stress (σ_{ij}) and strain behavior of the bird using the pressures observed at impact.

$$\sigma_{ij} = -P\delta_{ij} + 2\rho\gamma_v\dot{e}_{ij} \tag{7}$$

where δ_{ij} and $\dot{e}_{ij}$ represent the identity and rate-of-deformation tensors, respectively, P represents the fluid pressure, and γ_v represents the dynamic viscosity coefficient (Mao et al., 2007). By using the combined deviatoric material response and the hydrodynamic constitutive law, the material behaves like an elastic-plastic material at low pressures and follows a pressure-volume relationship during high velocity impacts (Hedayati & Sadighi, 2016). A low value of shear strength is often defined to allow the material to retain its shape until the impact. Based on numerical investigations performed by Airoldi, the yield stress for the bird material should be lower than 0.1 times the stagnation pressure of an incompressible fluid with the same density as the bird (Airoldi & Cacchione, 2006). In the second stage of the bird impact, the material flows causing rise to shear and tensile stresses. To properly simulate the flow of the material a hydrostatic cut-off stress (positive in tension) is also defined to permit the bird resisting a small amount of tension.

2.3.1 Equation of State (EOS)

The formulation of an EOS is necessary to model the impact behavior of a soft body on to a target. The EOS approach allows the modelling of a hydrodynamic pressure-volume relationship. No analytical approach for an EOS currently exists for solids and liquids. Many EOSs have been proposed in literature using semi-empirical formulas based on experimental data (Hedayati & Sadighi, 2016). For bird strike applications, common EOSs include the linear, polynomial, tabulated and the Mie-Grüneisen models.

Tabulated EOS models provide greater flexibility in modeling the hydrodynamic behavior of bird impacts. In the analyses performed in this report, Abaqus/Explicit was used. In a study by Dassault Systèmes, the recommended way to model bird impacts in Abaqus/Explicit was by using the tabulated EOS approach (SIMULIA, 2011).

The Hugoniot curves for water-like homogenized bird materials can be used as input for the Abaqus tabulated EOS (SIMULIA, 2011). The tabulated equation of state form is given below.

$$P = f_1(s_{vol}) + \rho_0 f_2(s_{vol}) E_{int} \tag{8}$$

In the tabulated EOS model, $f_1(s_{vol})$ and $f_2(s_{vol})$ are functions of the logarithmic volumetric strain s_{vol}, where $s_{vol} = ln\left(\frac{\rho_0}{\rho}\right)$. When dealing with the hydrodynamic region of impact, the internal energy contribution E_{int} can usually be neglected. Hence, the EOS reduces to:

$$P = f_1(s_{vol}) \tag{9}$$

2.4 Bird Mass and Density

In recent finite element studies, the testing of a 4 lb. (~ 1.81 kg) bird for calibration purposes is common (Mao et al., 2007). The effect of heavier birds of 6 lb. (~ 2.72 kg) and 8 lb. (~ 3.63 kg) has also been investigated in literature (Mao et al., 2007). Most finite element studies have used statistical relationships developed by Budgey to determine the density and diameters of bird models (Budgey, 2010; Guida et al., 2011).

$$\rho_0 = (-0.063 \log(1000m) + 1.148) * 1000 \tag{10}$$

In equation (10), m represents the mass of the bird in kg, while ρ_0 represents the density (before impact) in kg/m^3. The diameter of the bird D can be calculated from the mass of the bird.

$$D = 10^{-1.095+0.335\log(m)} \tag{11}$$

Alternately, the diameter can be found using a fixed length-to-diameter aspect ratio (L/D) (Mao et al., 2007).

$$D = 2\left(\frac{m}{2\pi\rho_0}\right)^{\frac{1}{3}}\left(\frac{L}{D} - \frac{1}{3}\right)^{-\frac{1}{3}} \tag{12}$$

2.5 Bird Shape

It has been observed during experimental and numerical analyses that the bird diameter can have a significant effect on the pressure history observed in an impact. Traditionally, three different geometrical shapes have been employed for analyzing bird impact using finite elements. These include the straight-ended cylindrical shape, the hemispherical-ended cylinder, and the ellipsoid. Recently, researchers have also studied the effectiveness of using bird shapes that more closely represent actual bird geometries. CT scans of actual birds have been used in finite element analyses (Hedayati, 2016). Such models representing the bird shape more closely, show better correlation with experimental results than those obtained by the traditional geometrical shapes.

However, reasonably accurate results may also be obtained from using traditionally shaped bird models.

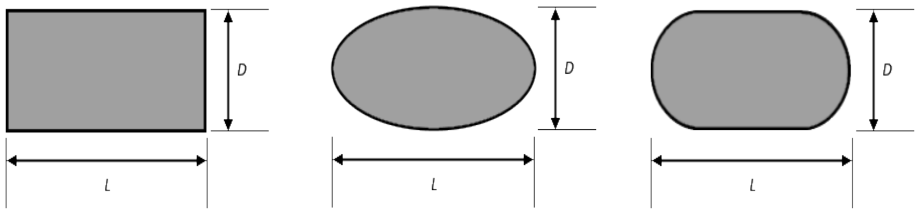

Figure 3: Traditionally shaped bird substitute models.

3. Fan Blade Model

Modern engine fan blades are made of titanium alloy Ti-6Al-4V. More recently, composite fan blades have also been used. Upon impact, the fan blade experiences high plastic deformations both locally (in the impact region) and globally (Mao et al., 2007; Selezneva et al., 2010). As the bird impact is a highly dynamic event, strain rate effects need to be addressed in the material model for the fan blade.

In the study presented in this paper, the Johnson-Cook plasticity model was used to account for the plasticity hardening and rate-dependent behavior. Within Abaqus/Explicit, the model can be used in conjunction with the Johnson-Cook dynamic failure model. Furthermore, at high impact velocities the material behavior can be better represented using an equation of state. Thus, for Ti-6Al-4V the Mie-Grüneisen EOS was used to model the material behavior when subjected to high velocity impact.

Table 1: Material properties for titanium alloy (Wang & Shi, 2013; Lesuer, 2000).

	Melting Temperature θ_{melt}, °C	Density ρ, kg/m^3	Heat Capacity c_{heat}, J/kg°C	Shear Modulus G, GPa	Inelastic Heat Fraction v_{heat}	Fracture Energy G_f, kN/m
Ti-6Al-4V	1605	4428	560	41.9	0.9	49.43

Table 2: Johnson-Cook damage parameters for titanium alloy (Lesuer, 2000).

	A_{JC}, MPa	B_{JC}, MPa	n	C_{JC}	m_{JC}	D_1	D_2	D_3	D_4	D_5
Ti-6Al-4V	1098	1092	0.93	0.014	1.1	-0.09	0.25	-0.50	0.014	3.87

Table 3: Mie-Grüneisen parameters for Ti-6Al-4V (Wang & Shi, 2013).

	c_0, m/s	k	γ_0
Ti-6Al-4V	5130	1.028	1.23

3.1 Blade Geometry

The fan blade geometry is dictated largely by aerodynamics. As the main purpose of the engine is to provide thrust to the aircraft, there is very little room for geometric modification of the blade as this may compromise its aerodynamic efficiency. Furthermore, aircraft components must be as light as possible and the addition of reinforcements to handle impact must also consider weight limitations. However, the internal thickness of the blade as well as the material it is constructed from may be optimized so that better damage tolerance is achieved.

4. Simulation Methodology

The simulations were performed in various stages using the Abaqus/Explicit solver. In the first set of simulations, the Lagrangian and SPH techniques were used to model the impact of a straight-ended cylinder onto a rigid target. These simulations were conducted to test the validity of the simulation parameters and controls. The results were compared with theoretical and experimental results available in literature. It must be noted that in this paper, the term bird is often used to refer to the bird substitute model.

Once the numerical techniques were validated, the chosen modeling technique was used to perform simulations using modified bird shapes. This part of the study was done to determine a calibrated bird model. The results were validated with those available in literature.

The calibrated bird model was then tested for impact on a flat titanium blade-like geometry. The thickness, chord, and the twist of the blade were varied to study the effects on energy absorption. The effects of the blade's rotational velocity on impact were also studied. Finally, the blade's geometrical properties were varied to study the effect of geometrical configurations on the energy absorption during impact. The following sections describe in more detail each part of the process.

4.1 Bird Model

As commonly suggested in literature, a length-to-diameter ratio of 2.0 was used for the cylinder (Hedayati & Sadighi, 2016). A density of 938 kg/m^3 was used with a mass of 1.814 kg to compare the results directly with the simulations performed by SIMULIA (SIMULIA, 2011). A cylinder length of 0.2144 m and diameter of 0.1072 m was used for the simulations. Non-porous gelation EOS was used to specify the material properties of the cylinder. An impact velocity of 200 m/s was used to compare with the results produced by Airoldi and SIMULIA (Airoldi & Cacchione, 2006; SIMULIA, 2011). As suggested by the SIMULIA guide, the yield stress of the bird material was chosen to be 0.1 MPa and its elastic strain limit was chosen to be 1%. Thus, a shear modulus of 10 MPa was used for the bird material (SIMULIA, 2011). To deal with material flow during the steady flow stage of the impact, a tensile failure value was specified, which acts as the hydrostatic cut-off stress. As suggested in literature, a 2.75 MPa stress was used as the tensile failure limit (Airoldi & Cacchione, 2006; SIMULIA, 2011).

Table 4: Bird properties used for the validation test.

Mass m, kg (lb)	Initial Density ρ_0, kg/m^3	Porosity z	Yield Stress $\bar{\sigma}$, MPa	Shear Modulus G, GPa	Hydrostatic Cut-off Stress σ_{HCO}, MPa	Length L, m	Diameter D, m	Impact Velocity u_0, m/s
1.814 (4)	938	0%	0.1	0.01	2.75	0.2144	0.1072	200

4.1.1 Lagrangian Model

The Lagrangian cylinders were modeled with linear hexahedral C3D8R (continuum, 3D, 8-noded, reduced integration) elements using enhanced hourglass stiffness. To deal with excessive deformation, the bird elements were deleted from the simulation once their equivalent shear plastic strain had exceeded 400% (SIMULIA, 2011).

4.1.2 SPH Model

Within Abaqus, the SPH method can be used by first defining the 3D geometry using Lagrangian finite elements (C3D8R used in this project) and then converting these elements at the beginning of the analysis to particles (SIMULIA, 2015). The conversion of elements can be handled in two ways. The traditional method in Abaqus is to generate a number of particles per parent element. This technique however can be troublesome as element density can vary for a complex part. Although the straight-ended cylinder is simple in shape, other geometrical shapes used to model the bird may have a lot of curvature which may result in more particles being generated near areas of changing curvature. Since each particle in the SPH method has the same mass, the particles per parent element approach can result in uneven mass distribution of the underlying solid. The second approach in Abaqus generates a uniform distribution of particles and thus the results are more accurate. This is the recommended approach and was preferred in this project. For the SPH based simulations, there were no distortion controls or element deletion parameters specified as particles don’t suffer from the distortion problems of Lagrangian elements. Zero-energy modes like hourglassing can also occur with the SPH method, however, it is highly unlikely for these modes to be found in regular SPH simulations as they occur only in very particular cases (Liu & Liu, 2003). Thus, hourglassing was not considered in the SPH simulations.

4.2 Plate Model

The plate was modeled as a fixed rigid steel plate using S4R shell elements. The overall plate dimensions were chosen to be 10 m by 10 m so that the deformed bird shape is completely captured by the plate. The plate was progressively meshed such that the center of the plate had elements measuring 0.005 m in length. Four elements around the center of the plate were used to calculate the peak impact and stagnation pressures as suggested by Airoldi and the SIMULIA guide (Airoldi & Cacchione, 2006; SIMULIA, 2011). Physically this Hugoniot area corresponded to a 0.01 m by 0.01 m area on the rigid plate. However as described in the SIMULIA guide, Abaqus extrapolates the specified area to a 0.015 m by 0.015 m to account for load areas of the nodes located on the perimeter of the surface (SIMULIA, 2011). Similarly, an area of 0.21 m by 0.21 m centered about the plate's center to capture the steady flow was defined. All impact forces were derived from this area.

4.3 Contact Assignment

To handle contact, the general contact algorithm available in Abaqus was used with the penalty contact formulation. Contact between the Lagrangian cylinder model and the plate was specified for all interior and exterior element faces of the cylinder. Self-contact was also defined for the cylinder. A frictionless interaction property was defined as friction does not play a significant role during high-speed bird impacts and the addition of friction would have significantly increased the computation time. In Abaqus, if the general contact definition is applied on the Lagrangian elements, upon conversion all SPH particles will automatically inherit the contact definitions. Thus, for the SPH based simulations, a general contact definition along with self-contact was sufficient.

4.4 Stabilization Parameters

Impact analyses can have a lot of noise and may lead to convergence issues due to high deformations. A critical damping fraction of 0.4 was used in Abaqus/Explicit to smoothen the response.

5. Results

5.1 Validation Testing

The results from the Lagrangian and SPH simulations were found to be very similar and they matched well with those published in literature. The SPH approach was found to be better than the Lagrangian method because mesh distortion is not applicable to SPH models. Thus, slashing behavior of the bird can be modeled more efficiently using the SPH method. When modeling using the SPH methodology, a uniform distribution of particles is necessary. This is so the mass of an underlying homogeneous body is equally distributed. Furthermore, an upper limit on the number of particles used to model a bird geometry should be specified. This is because too many particles cluttering in one location can lead to the tensile instability phenomenon in SPH based simulations.

5.2 Calibration of Bird Material and Model

The results from the calibration study showed that there is a significant effect of the shape of the impacting projectile on the force-time history. The straight-ended cylinder model showed very high force magnitudes at the beginning of impact and a sharp drop in the magnitude following the initial phase of the impact. Comparatively, the hemispherical-ended cylinder and ellipsoid shapes showed a smoother variation in the force magnitude and more closely resembled the force-time histories obtained by Barber and Wilbeck using real chicken carcasses (Barber et al., 1978; Wilbeck, 1977).

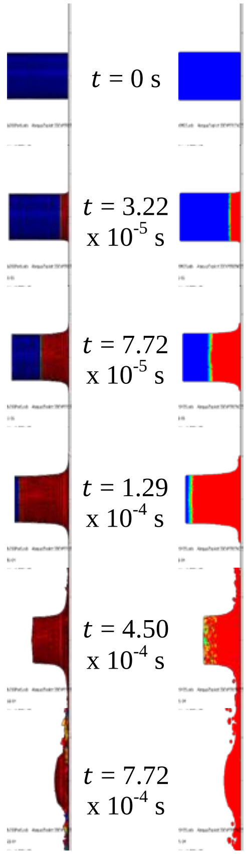

Figure 4: Side view for the converged validation impact tests using the Lagrangian (left) and the SPH (right) approaches. The shockwave can be seen propagating through the model at various stages of impact.

The ellipsoid and hemispherical-ended cylinder for 10% and 15% porosities had results that were close to the average of experimental results. The results also showed that increasing the curvature of a projectile would shorten the duration of the shock pressure. Furthermore, increasing porosity was found to lower the peak impact pressure. In general, the SPH based simulations were found to have higher observed peak pressures than those obtained from the Lagrangian approach. Based on the results, the SPH based method using a hemispherical-ended cylinder with 10% porosity was used as the calibrated bird material and model. Finally, an aspect ratio of 1.6 was found to match the theoretical results more closely than aspect ratios of 2 and 2.94.

As seen from Figure 6, the calibrated (or current) model used in this project has a history very similar to that published by Airoldi and SIMULIA. The peak pressure seems to be slightly higher than that published by Barber and Wilbeck, which can be attributed to the limitations of the pressure transducers used by Barber and Wilbeck (Barber et al., 1978). The transition between the peak pressure and the steady-flow pressure seems to be smoother for results obtained using simulations, while for the experimentally obtained history by Barber and Wilbeck, the transition is more sudden. In general however, the pressure-time history correlates well with the experimental results.

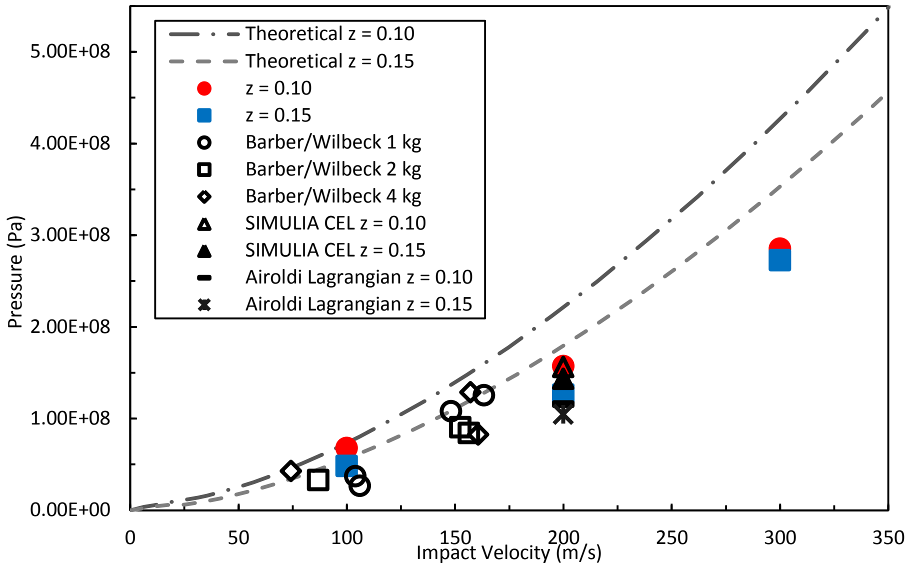

Figure 5: Hugoniot pressure plot is shown. The results for a hemispherical-ended cylinder with L/D ratio of 1.6 are compared with theoretical and published data.

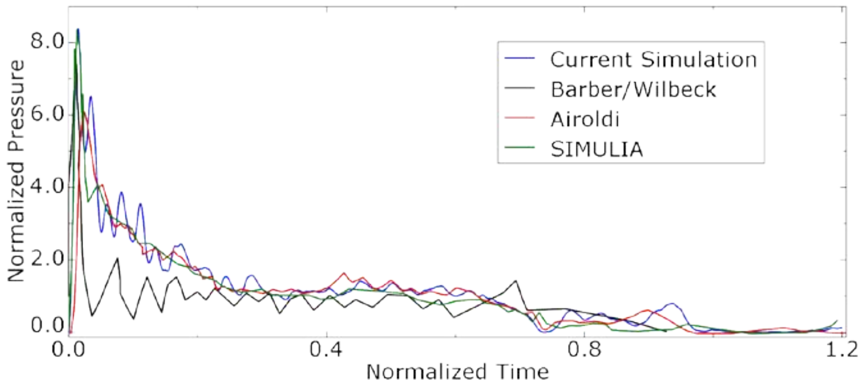

Figure 6: Normalized pressure vs. time graph is shown for the calibrated hemispherical-ended cylinder using the SPH approach using gelatin with 10% porosity as the material. The results have been compared with published and experimental data (Barber et al., 1978; Airoldi & Cacchione, 2006; SIMULIA, 2011).

5.3 Impact on a Non-Rotating Blade

Based on the results obtained, an increase in blade length was found to decrease the maximum plastic strain and maximum displacement observed during impact. An increase in the blade width was found to increase the maximum plastic strain observed in the blade, while decreasing the maximum displacement observed in the blade. Increasing the thickness of the blades was found to have a positive effect on the impact resistance of the blade. Both maximum observed plastic strain and maximum observed displacement values were found to decrease with increasing thickness. It was also observed, that the hollow corrugated triangular blade had lower impact resistance than the solid blades. In the simulations performed for the current study, the maximum plastic strain found in the hollow blade was over three times higher than the maximum plastic strain observed in a solid blade of similar dimensions. Furthermore, for the hollow blade the maximum plastic strain was found to be near the impact location, in the core. For the solid blade, the maximum plastic strain was found to be slightly away from the impact zone near the leading edge of the blade.

Various blade twist angles were considered to understand the effect of twist on impact behavior. It was found that as the twist of a non-rotating blade increases, the maximum plastic strain and maximum displacement also increase. Finally, the impact of large bird simulations found that there is an increase in both the maximum plastic strain and maximum displacement observed as the mass of the impacting bird is increased.

5.4 Impact on a Rotating Blade

To study the impact behavior on rotating blades, the centrifugal effect on the blade was first simulated using Abaqus/Standard. This allowed the blade to be in a pre-stressed state (due to rotation) after which the impact simulations were performed. The results showed that the plastic strains for the rotating cases are higher than the plastic strains obtained for non-rotating cases. Furthermore, the plastic strains were found to decrease with increasing twist for the rotating cases. Particularly, it was found that a larger slice of the bird due to blade rotation contributed to larger plastic strains. The damage for rotating blades was found to be localized near the impact zone.

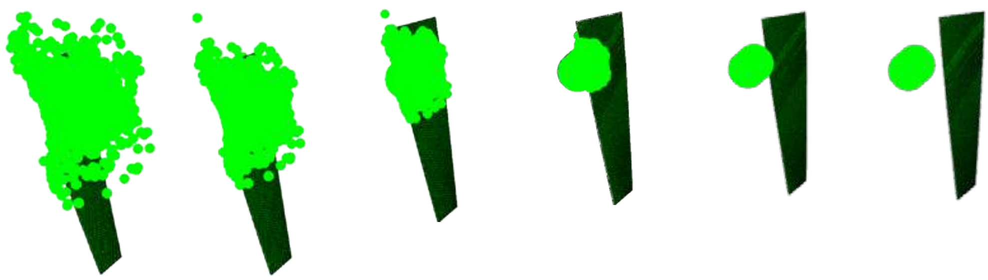

t = 5.53 x 10^{-4} s	t = 4.42 x 10^{-4} s	t = 3.32 x 10^{-4} s	t = 2.21 x 10^{-4} s	t = 1.11 x 10^{-4} s	t = 0 s

Figure 7: Impact progression of a rotating blade (from right to left). A blade with 67.5° twist is shown in the image with the side impact configuration.

6. Conclusions

Bird strikes are an important phenomenon that must be considered when designing aircraft engines. This report summarizes the work done to understand and analyze the behavior of bird strikes on engine blades. The intent of this project was to find an acceptable bird substitute model that can be used in finite element based simulations so that expensive physical testing can be reduced or replaced. Furthermore, engine fan blade optimization purely from an impact resistance perspective was also studied. Particularly, the SPH method was found to be both efficient and accurate in modeling a bird impact event compared to a Lagrangian approach. The twist for rotating engine blades was found to have a beneficial effect on impact tolerance. Finally, as the impact is localized during a high-speed impact on a rotating blade, areas away from the leading edge of the blade can be made of light composite or sandwich structures to minimize weight.

Significant room for research exists in understanding bird strikes and bird strike damage. Most of the data which is available on bird strikes is old and the pressure sensors used to obtain the data were not ideally suited for measuring the stresses due to bird strikes. Thus, there is a need to perform new physical experiments to obtain impact pressures due to bird strikes. Furthermore, different bird species should be tested for impact. Most experimental data available today has been obtained using chicken carcasses or gelatin capsules, while larger birds like the Canada goose pose a greater threat as far as bird strikes are concerned. A multi-material model of the bird taking to account bones, muscles, skin, and flesh would give a better representation of a bird strike. With regards to the design of engine blades, bird impact simulations on various configurations of the sandwich core can be performed. Composite materials are another area of research that should be thoroughly studied in future bird strike simulations. Another possible area of research can be in evaluating the post-damage response of an engine blade after a bird impact.

7. References

[1] U.S. Department of Transportation, "Wildlife Strikes to Civil Aircraft in the United States 1990-2012," in *Federal Aviation Administration*, Washington, DC, 2013.

[2] E. C. Cleary, R. A. Dolbeer and S. E. Wright, "Wildlife Strikes to Civil Aircraft in the United States 1990-2004," Federal Aviation Administration National Wildlife Strike Database, 2005.

[3] J. P. Barber, H. R. Taylor and J. S. Wilbeck, "Bird Impact Forces and Pressures on Rigid and Compliant Targets," University of Dayton Research Institute, Technical Report AFFDL-TR-77-60, Dayton, OH, 1978.

[4] J. S. Wilbeck, "Impact Behavior of Low Strength Projectiles," Air Force Materials Lab, Air Force Wright Aeronautical Labs, Report No. AFML-TR-77-134, Wright-Patterson AFB, OH, 1977.

[5] S. Heimbs, "Computational methods for bird strike simulations: A review," Computers and Structures, vol. 89, pp. 2093-2112, 2011.

[6] F. J. Heymann, "On the Shock Wave Velocity and Impact Pressure in High-Speed Liquid-Solid Impact," *Transactions of the ASME (Journal of Basic Engineering),* vol. 90, no. 3, pp. 400-402, 1968.

[7] A. Airoldi and B. Cacchione, "Modelling of impact forces and pressures in Lagrangian bird strike analyses," International Journal of Impact Engineering, vol. 32, pp. 1651-1677, 2006.

[8] R. H. Mao, S. A. Meguid and T. Y. Ng, "Finite Element Modeling of a Bird Striking an Engine Fan Blade," *Journal of Aircraft,* vol. 44, no. 2, pp. 583-596, March-April 2007.

[9] R. Hedayati and M. Sadighi, Bird Strike: An Experimental, Theoretical, and Numerical Investigation, Cambridge: Elsevier Ltd., 2016.

[10] SIMULIA, "A Strategy for Bird Strike Simulations using Abaqus/Explicit," Dassault Systèmes, 2011.

[11] R. Budgey, "The Development of a Substitute Artificial bird By the International Birdstrike Research Group for Use in Aircraft Component Testing," in *International Bird Strike Committee*, Amsterdam, 2000.

[12] M. Guida, F. Marulo, M. Meo, A. Grimaldi and G. Olivares, "SPH – Lagrangian study of bird impact on leading edge wing," *Composite Structures*, vol. 93, no. 3, pp. 1060-1071, 2011.

[13] M. Selezneva, P. Stone, T. Moffat, K. Behdinan and C. Poon, "Modeling Bird Impact on a Rotating Fan: The Influence of Bird Parameters," in *11th International LS-DYNA Users Conference*, Dearborn, 2010.

[14] X. Wang and J. Shi, "Validation of Johnson-Cook plasticity and damage model using impact," *International Journal of Impact Engineering*, vol. 60, pp. 67-75, 2013.

[15] D. R. Lesuer, "Experimental Investigations of Material Models for Ti-6Al-4V Titanium and 2024-T3 Aluminum," Federal Aviation Administration, DOT/FAA/AR-00/25, Livermore, 2000.

[16] SIMULIA, Abaqus Analysis User's Guide (Volume III), Dassault Systèmes, 2015.

[17] G.-R. Liu and M. B. Liu, Smoothed Particle Hydrodynamics: A Meshfree Particle Method, Singapore: World Scientific, 2003.

8. Acknowledgements

I wish to express my deep gratitude and appreciation for Dr. Shaker Meguid of the University of Toronto, who supported me in the research and implementation of this project.